Journal of Paleolimnology (2005) 33: 327–347

Distinguishing climatic from direct anthropogenic influences during the past 400 years in varved sediments from Lake Holzmaar (Eifel, Germany)

Ulrike Kienel*, Markus J. Schwab and Georg Schettler
*GeoForschungszentrum Potsdam, Section Climate Dynamics and Sediments, Telegrafenberg C327, 14473 Potsdam, Germany; *Author for correspondence (e-mail: ukienel@gfz-potsdam.de)*

Received 2 May 2004; accepted 21 October 2004

Key words: Correspondence analysis, Diatoms, Fuzzy clustering, Historical data, Little Ice Age, Maar lakes, Sunspot minima, Varves

Abstract

A 336-year floating varve chronology from Lake Holzmaar (Eifel, Western Germany) covering the recent period has been established by microfacies analysis of thin sections. This sequence terminates 23 cm below the core top. In the top 23 cm, the varves are disturbed. By means of linear regression, the varve sequence was dated to the period AD 1607–1942. The influences of climatic variability and anthropogenic activities in the lake's catchment (e.g., forestry, agriculture) on lithology, fabric, and microfossil content of the varve sublaminae could be discriminated by applying statistical analyses (ordination and clustering) to the combination of the sublaminae in the varves and their thickness. Four clusters are obtained. Cluster 1 indicates cold springs, and shorter, cooler summers reflected primarily in below-average varve thickness (VT) for two stable phases: from AD 1650–1700 (during the Maunder Minimum) and from AD 1750–1785. Cluster 2 indicates years with conditions transitional to that indicated by cluster 1, characterized by vigorous and prolonged spring circulation with massive blooms of the nordic-alpine *Aulacoseira subarctica*. The samples assigned to Cluster 3 and Cluster 4 show the imprint of anthropogenic influences. Cluster 3 (AD 1795–1815 and AD 1825–1885) is characterized by above-average VT due to high detritus input throughout the year. The increased soil erosion can be linked to anthropogenic deforestation as a consequence of the production increase of the Eifelian iron industry at the end of the 18th century. This input dampens the climatic signal of a colder Dalton Minimum, which is reflected in a short drop in VT centered around AD 1810. At about AD 1885, Cluster 4 conditions, characterized by increased nutrient concentrations, low detritus input, and longer periods of stable summer stratification, become the stable state in Lake Holzmaar. They indicate the response of the lake to natural reforestation and the use of artificial fertilizers in the catchment, which began, according to historical records, in the 1850s in the Eifel region. The prolonged, stable summer stratification periods may be the first indication of the modern warming trend. A drop in VT centered around AD 1890 and recurring cluster-1 conditions may indicate the Damon Minimum.

Introduction

Among the consistently discussed problems in limnogelogical studies of sequences covering the historic period is the distinction between the climatic and anthropogenic influences (e.g., Hausmann et al. 2002; Lotter and Birks 1997; Tinner et al. 2003). This relates on the one hand to

lake management and lake restoration from eutrophication or acidification and on the other hand to the attempt to reconstruct the natural versus anthropogenic induced climate variability.

Climate variability of the past four centuries in Europe is well documented in instrumental and documentary records (e.g., Manley 1974; Eddy 1976; Pfister 1999; Glaser 2001). Indirect methods are used to supplement the instrumental data, such as the number of sunspots. These show distinctive minima termed the Maunder Minimum (MM: AD 1645–1715), the Dalton Minimum (DM: AD 1795–1825) and the Modern or Damon Minimum (DoM centered at about AD 1900) (Eddy 1976; Jones 1988; Hoyt and Schatten 1998; Bard et al. 2000). The MM, where almost no sunspots were observed, delineates the coldest phase of the 'Little Ice Age' in Europe (LIA, AD 1300–1900) (e.g., Pfister 1999; Glaser 2001) coinciding with reduced solar activity (Lean and Rind 1999), enhanced atmospheric ^{14}C (Stuiver and Braziunas 1993), and large volcanic eruptions (Briffa et al. 1998). Compilations of historical and early instrumental data (Jones 1988; Pfister 1999; Glaser 2001) show that the cooling first influenced the British Islands followed by central and eastern Europe. According to the same authors, the strongest temperature decreases were recorded in the winter periods (5–6 °C), while the temperatures in the autumn periods showed the least negative deviation. The summers from AD 1694–1700 were the coldest in the present millennium (Jones et al. 1998). The winter temperature decrease (DJF) during the period AD 1675–1715; as reconstructed from early instrumental data, documentary evidence and from natural archives (Zorita et al. 2004); shows regional differences. Departures of more than 1.2 °C were reconstructed for Eastern Europe, around 1 °C for Central and Western Europe, and up to 0.5 °C for the Mediterranean, the British Islands and Southern Scandinavia. Less negative temperature deviations were reported for the DM and for the DoM (Jones 1988; Pfister 1999; Glaser 2001).

The prerequisite for discussing interactions of climatic and anthropogenic influences on lacustrine sediments is an accurate chronology as it offers the opportunity for comparison between reconstructions from archives and the instrumental and historical data. Annually laminated (varved) sequences provide the highest accuracy and seasonal resolution (Anderson and Dean 1988; Glenn and Kelts 1991; Brauer 2004). Variability of the lacustrine sedimentation, as a result of external and internal influences on the lake, may be observed in great detail (Lotter 1998; Alefs and Müller 1999; Merkt and Müller 1999). Sediment trap studies indicate that thermal regimes and trophic states are factors that could potentially be recorded in lacustrine varves of biogenic-clastic composition (Bradbury 1988; Raubitschek et al. 1999). Together with catchment characteristics and precipitation, the thermal regime influences the allochthonous sedimentation. A seasonal plankton succession related to the trophic state of the lake determines the autochthonous deposition (Sommer et al. 1986). According to the PEG-model (Sommer 1988), blooms of phytoplankton in lakes begin with species that are adjusted to lower light availability i.e. under the ice or during spring circulation. Most diatom species develop blooms once the mixing depth is reduced to a point where they remain in the photic zone. Such small, fast growing centric diatoms are grazed by a rapidly developing zooplankton population. During summer stratification occur only species that are not grazed by the zooplankton because of their large size (Sommer 1988). With decreasing temperatures and increasing mixing depth in late-summer, the nutrient pool of the lake is refilled and a second diatom bloom occurs. This bloom of mainly large centric species that are adjusted to lower light availability, is often grazed during a second zooplankton maximum.

With information concerning these successions and their signature in the sediment, the sublaminae observed in the varves can often be assigned to the season of their formation. In biogenic-clastic varves, one can distinguish diatom-bloom layers and clastic/organic layers (e.g., Baier et al. 2004) that may be accompanied by calcite precipitates (e.g., Lotter 1989; Lotter et al. 1997). The preserved diatoms are important indicators for changes in environmental variables, such as nutrient concentration, water pH, temperature (thermal regime) and other factors (e.g., Stoermer and Smol 1999; Battarbee 2000; Ramstack et al. 2003; Siver et al. 2003; Bradbury et al. 2004). In addition to the accurate chronology, the detailed information from the seasonal sublaminae make varved sediments one of the favored proxy data archives for

climatic and environmental reconstructions (e.g., Itkonen and Salonen 1994; Ohlendorf et al. 1997; Wohlfarth et al. 1998a; Smith et al. 2004).

Apart from glacier-fed lakes, maar lakes are well known for the preservation of varved sediments. Lake Holzmaar in the Eifel region (Germany), for example, provides a varved record extending back to 23,220 calendar years BP (Zolitschka et al. 2000). Studies of individual periods, covering the period 23,220–2220 calendar years BP, show that this varved record provides information in great detail on climatic development (Zolitschka and Negendank, 1998; Brauer et al. 2001) and human activities (Zolitschka 1998; Baier et al. 2004) in the region.

The objectives of this study are to: (i) establish a varve chronology covering the recent period of varved sedimentation in Lake Holzmaar; this is done using microfacies analysis of varves in thin sections with special emphasis to the preserved diatoms, their seasonal distribution and ecological preferences; (ii) relate features in the varve microfacies to climatic or anthropogenic influences; this is done by statistical analysis of the combination of sublaminae and their thickness in each varve and by comparison of this results with data from local and regional historical documents, north hemispheric instrumental data and climate reconstructions.

Study Site

Lake Holzmaar is situated in the West Eifel Volcanic Field (Germany) at 50°7′N, 6°53′E, 425 m a.s.l. (Figure 1). Morphometric and hydrological data are given in Table 1. The inlet and outlet of the lake are formed by a brook passing by the main basin via a shallow embankment area in the southwest. Apart from that, Lake Holzmaar is circular in shape. The maar was formed by phreatomagmatic eruptions ca. 40,000–70,000 years ago (Büchel 1993). Arable land comprises 60% of the present-day catchment; the remaining area and the crater wall are forested predominantly by beech (*Fagus sylvatica*).

The water pH is 9 on average, but can exceed 10 in the epilimnion during summer stratification (fortnightly measurements of depth profiles, Lücke et al. 2003). Total phosphorus concentrations (18–22 $\mu g\ l^{-1}$) in the top 10 m of the water column in the lake center classify the lake as oligo-mesotrophic. The electrical conductivity is low (197–303 $\mu S\ cm^{-1}$) (depth profiles measured in each case in March 1993–2001 by the Landesamt für Wasserwirtschaft Rheinland-Pfalz). The lake is predominantly dimictic and holomictic (Thienemann 1915; Scharf and Oehms 1992). However, during summer stratification, Lücke et al. (2003) observed anoxic conditions for the hypolimnion below 12 m depth.

Table 1. Morphometric and hydrological data of Lake Holzmaar and its catchment (Scharf and Menn 1992).

Variable	Value
Altitude of lake level [m a.s.l.]	425.1
Maximum water depth [m]	20.0
Mean water depth [m]	8.8
Lake surface area [m^2]	58,000.0
Catchment area [m^2]	2,058,000.0
Water volume [m^3]	510,000.0
Length of shore line [m]	1100.0
Theoretical water retention time [a]	0.6
Maximum elevation in the catchment [m a.s.l.]	477.0

Local climate data for the last few decades are from the closest weather station of the 'Deutscher Wetterdienst' (German weather service) in Manderscheid (in Figure 1, Table 2). Compared to the longterm mean (1961–1990), the data for the period 1985–2001 show increased values for all temperature categories, annual precipitation and the monthly precipitation maxima.

According to a 1995 sediment trap study of diatom development in relation to temperature and silica concentrations, diatom growth started in late-April (Raubitschek et al. 1999). Both the spring bloom in late-May through June, and the fall bloom from mid-August through October, were dominated by *Cyclotella comensis* Grunow. A short, less pronounced summer bloom of *Fragilaria crotonensis* Kitton occurred in the second half of July. In May and from September onwards, higher trapping rates of littoral diatoms in the deepest trap (traps in 3, 6 and 16 m water depth) suggested minor sediment focusing or resuspension of littoral sediments, respectively.

Material and methods

The surface core HZM 41 was recovered by gravity coring using the Ghilardy Freefall Corer

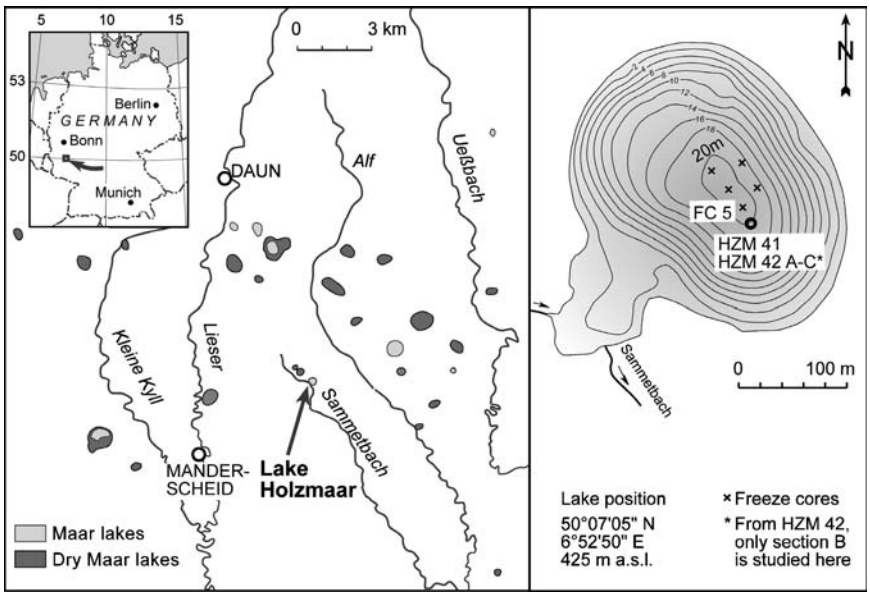

Figure 1. Lake Holzmaar. Location, catchment, bathymetry and core position.

(Kelts et al. 1986). The sediment surface was documented as intact with clear water on top in the plastic tube. The core HZM 42 was retrieved close to HZM 41 (Figure 1) using a UWITEC Piston corer (http://www.uwitec.au). Sections HZM 41 (coring depth: 0.0–1.075 m) and HZM 42B (coring depth: 1.025–2.03 m), both recovered in summer 1999, are the focus of the current study.

The sediment shows distinct laminations with beige to olive and brown to dark brown colors. The alternating sublaminae consist of silt with changing portions of fine organic detritus, and diatom ooze. Intercalated clastic turbidites grade from fine sand to clay at the top and contain remains of plant macrofossils (classification according to Schnurrenberger et al. 2003). The section is varved throughout, except for the top 23 cm, where the laminae are disturbed. Five freeze cores (Figure 1), recovered in 1999, using a UWITEC Freeze corer type 4, consistently showed this pattern. The depth at which the varved section terminated varied from 10 to 31 cm. Given the freeze core results and the intact surface of the gravity core, it appears that the disturbance of the lamination is unrelated to coring.

The mean sedimentation rate for sediments of the top 37 cm was estimated based on ^{210}Pb-measurements. One cm sample slices were analyzed from the top 17 cm of the freeze core FC5 (the upper, unconsolidated sediments) and between 10 and 37 cm depth of core HZM 41. The activity of supported ^{210}Pb was measured by

Table 2. Local climate data from Station Manderscheid (50°6′ N; 6°48′ E; 403 m a.s.l.) (data from 'Deutscher Wetterdienst' (German Weather Service).

Station Manderscheid	Temperature means [°C]		Precipitation [mm]		
			Mean annual sum	Monthly maxima	
Longterm mean (1961–1990)	Annual	7.5	846.0	December	85.0
	July	16.0		January	85.0
	January	− 1.0			
(1985–2001)	annual	8.4	974.8	December	123.2
	July	17.0		January	110.8
	January	0.3			

γ-spectrometry of short-lived ^{226}Ra daughter nuclides [^{214}Pb (295.21 keV), ^{214}Pb (331.92 keV), and ^{214}Bi (609.31 keV)] in a Germanium well-type detector. Sample aliquots of 1–2 g freeze dried sediment were stored in gas-tight sealed quartz tubes for four weeks before measurement. Total ^{210}Pb activities of the freeze core samples were determined by α-spectrometric measurement of ^{210}Po (preparation according to Flynn (1968)). Total ^{210}Pb in samples from the gravity core HZM 41 was determined by γ-spectrometry.

A series of overlapping thin sections was prepared. Shock-freezing, freeze-drying and impregnation with epoxy resin were applied to sediment blocks ($100 \times 20 \times 20$ mm) before they were mounted, sawed by microtome and ground to a thickness of approximately 40 μm.

For light microscopy of the thin sections, a Zeiss *Axioskop 2 plus* microscope equipped with polarisation was used with magnifications ranging between 25× and 630×.

The sublaminae within the biogenic/clastic varves of Lake Holzmaar are distinguished based on: color; fraction of organic and clastic detritus, grain size and mineralogy of the latter; fraction of diatoms, their specific life form or habitat, and their temporal occurrence in the seasonal plankton succession; and the fraction of chrysophyte cysts. The combination of the different seasonal sublaminae constitutes the "varve microfacies" (Figure 2).

For thickness and position determination of the sublaminae in the thin sections, the vernier values of the x- and y-directions of the cross stage were used, so that a direct relation to sediment depth could be established. This method guarantees the traceability of the results. In the case of layer boundaries deviating from the direction perpendicular to the measuring track, layer thickness was corrected for orthogonality such that the measured distance was multiplied by the cosine of the deviation angle. Gaps resulting from cracks formed during the preparation process were subtracted from layer thickness. For the estimation of the percentage of the different components in the varves, we utilized the diagrams, representing various percentages of grains, constructed by Shvetsov (1954), communicated by Terry and Chillingar (1955), and used in international projects, such as the Ocean Drilling Program (ODP).

Diatom species were identified within the thin sections by comparison with earlier studied diatom preparations (according to Renberg 1990) from the same core (Kumke et al. 2004) using standard literature for diatom taxonomy (Krammer and Lange-Bertalot 1986, 1988, 1991a, b).

The varve series was counted twice with a gap of approximately one year by the same analyst (UK). Both time series differed by one year, resulting in a counting error $<1\%$. As this difference is the consequence of the previous misinterpretation of one annual layer, the latest count has been used for the analyses.

From the studied core sections, five samples have been dated by AMS$-^{14}$C analyses in the Leibnitz Laboratory University Kiel (Table 3).

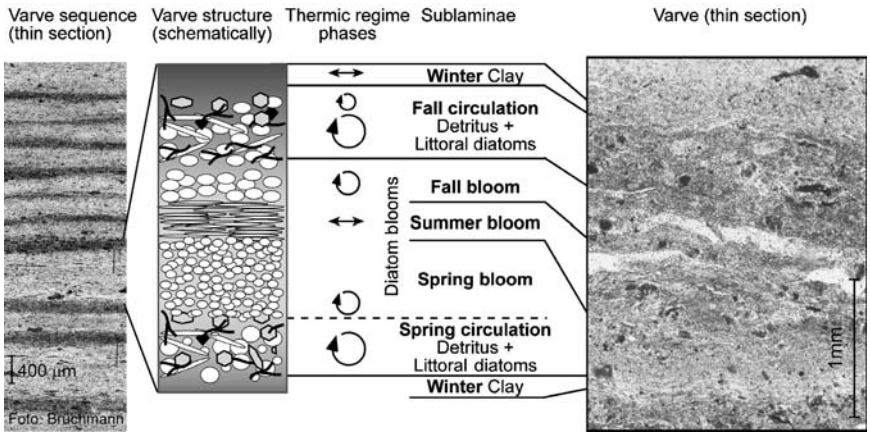

Figure 2. Varve texture, thin section image and sketch of a typical varve in the Holzmaar sequence.

Table 3. AMS ^{14}C dates of the Lake Holzmaar cores HZM41 and HZM42B.

Core HZM	Composite depth [cm]	Material (terrestrial)	Lab sample # KIA	^{14}C age [yr BP]	Corrected +/−	Calibrated 2σ cal BP		
						min	max	probability
42B	84.88	wood	11691	228	25	1640	1677	0.548
41	85.00	shrub wood	11688	44	25	1876	1917	0.556
42B	96.88	plant remains	11692	160	24	1723	1784	0.434
41	104.50	leaves	11689	322	30	1487	1643	1.000
42B	106.38	leaves	11693	196	25	1733	1807	0.623

The sample increment is 0.5 cm. The conventional age is defined according to Stuiver and Polach (1977), conventional dates are calibrated according to Stuiver et al. (1998) using CALIB REV4.4.2.

Statistical analyses

As the analysed thickness data from the varve sublaminae were right skewed and contained many zero values, they were transformed using $\ln(x + 1)$. Sublaminae with less than 10% occurrences in all annual layers were not considered because of their negligible influence on the results of the analyses (Table 4).

Statistical analyses comprised techniques of ordination and clustering. Detrended correspondence analysis (DCA; Hill and Gauch 1980) was applied in order to establish whether linear or unimodal ordination methods were suitable. DCA, with detrending by segments and non-linear rescaling, calculates the length of gradient that is expressed in the response variable. The gradient length is expressed in standard deviation units (SD) of species turnover. If the gradient length is short (<3 SD), linear methods are more appropriate, as for example, principal components analysis (Hotelling 1933, cited in Legendre and Legendre 1998). If the gradient length exceeds 3 SD, non-linear methods, such as correspondence analysis (CA; Hirschfeld, 1935, cited in Legendre and Legendre 1998), can be used to efficiently reduce the variability in the dataset to the main hypothetical gradients.

Table 4. Sublayer codes (CS), summary codes of bloom layers (CB): SB – spring bloom, SuB – summer bloom, FB – fall bloom, associated phase of thermic regime and numbers of occurrence (*N*).

Sublayer	CS	CB	Phase of thermic regime	*N*
Spring circulation	1SC		1 Spring circulation	208
Aulacoseira subarctica	*1Asu*	1SB		75
Spring input	1Sp			63
Stephanodiscus medius	*2Sme*	2SB	2 Terminating spring circulation	40
Cyclotella comensis	*2Cco*	2SB		36
Chrysophyte cysts	2CC	2SB		30*
Cyclotella pseudostelligera	*2Cps*	2SB		6*
Asterionella Formosa	*2Afo*	2SB		42
Fragilaria tenera	*3Fte*	3SuB	3 Summer stratification	77
Synedra ulna	*3Sul*	3SuB		3*
Fragilaria crotonensis	*3Fcr*	3SuB		1*
Chrysophyte cysts	3CC	3SuB		4*
Summer input	3Su			122
Aulacoseira subarctica	*4Asu*	4FB	4 Onset of fall circulation	21
Asterionella formosa	*4Afo*	4FB		5*
Chrysophyte cysts	4CC	4FB		1*
Cyclotella comensis	*4Cco*	4FB		36
Punctinella radiosa	*4Pra*	4FB		193
Fall indifferent	4F			83
Fall circulation	5FC		5 Fall circulation	305
Winter clay	6Wcl		6 Winter stratification	150

Sublayers whose *N*-value is marked by * do not pass the cut-off criterion of 10% occurrences. The number-code refers to the phase of thermal stratification under which the layer was deposited.

The interpretation of the data structure derived from a CA is mainly based on the arrangement of sample scores (here the year of the annual layer) and species scores (here the sublayers) in biplots by application of the distance rule (ter Braak 1994). DCA and CA were performed with the computer package CANOCO 4.5 (ter Braak and Smilauer 2002).

In order to find subsets with similar properties in the structure of the annual layers in the Holzmaar sequence, fuzzy c-means (FCM) cluster analysis (Bezdek et al. 1984) has been applied. This method has a wide field of utilization in the geosciences, whenever groups in multivariate datasets are required for interpretative or classification purposes e.g., in pedology (Hanesch et al. 2001) or in paleomagnetic studies (Dekkers et al. 1994). FCM clustering has been chosen here, because of its advantages for the analysis of geological datasets over conventional hierarchical clustering in general and over time-constrained clustering. The latter, because of the time constraint, cannot assign samples at different stratigraphical levels to one cluster, even though they fulfill the criterion of similarity. Thus, valuable information on recurring states in the sequence is lost. Additionally, and in contrast to common clustering, FCM clustering provides the opportunity for adjustment of the clustering to data that describe natural processes with gradual changes. The degree of fuzziness of the clustering can be increased by decreasing the value of the embedded membership function from 1 (identical with the cluster) to 0 (different from the cluster) and by increasing the fuzzy-exponent ϕ from 1 (conterminous with hard clustering) to ∞ (Bezdek et al. 1984). An additional advantage of the FCM clustering is that it includes the significance test. Because the clustering process starts from random samples, coincident results in repeated runs of the analysis are the test for significance and stability of the solutions (Vriend et al. 1988).

For determination of the validity of a subdivision into clusters, three validity functionals are calculated (Bezdek et al. 1984): the separation distance between the clusters (S_{dist}), the modified partition entropy (MPE), and the fuzziness performance index (FPI). The optimum number of the clusters is established on the basis of minimizing these three measures. Fuzzy c-means clustering was conducted using the software FuzME 3.5© Miasny, B., McBratney, A.B., http://www.usyd.edu.au/su/agric/acpa/fkme/program.html

Results

Fabric of the varves and sublaminae

We distinguished 21 sublayers in the varves of the Holzmaar sequence. According to both their succession within the annual layer and the combination of characteristic features (see Material and methods), the sublaminae were assigned to a season and phase of the thermal regime. (Table 4 – coding discussed below). The prefix number refers to the phase of the thermic regime during which the respective sublamina formed: 1 – spring circulation; 2 – termination of spring circulation; 3 – summer stratification; 4 – onset of fall circulation; 5 – fall circulation; and 6 – winter stratification.

The sublaminae containing the sediments of spring circulation (1SC) are characterized by predominantly allochthonous components: minerogenic and organic detritus comprising up to coarse-silt sized clastics, and plant remains of twigs, leaves, or roots. Pennate diatoms that are redeposited from their littoral habitat also occur frequently. In a number of years, a first diatom bloom of *Aulacoseira subarctica* (O.Müller) Haworth (1Asu = 1SB) already occurs during spring circulation. This is in accordance with the species' preference to well mixed waters and its tolerance to light deficiency (Interlandi et al. 1999; Reynolds et al. 2002). Ideally, the spring-circulation layer is overlain by mono- or duo-species layers of planktonic diatoms, attributed to spring-, summer- and late-summer or fall blooms.

Among the spring bloom laminae (2SB) are laminae of *Cyclotella comensis* Grunow (2Cco), *Asterionella formosa* Hassall (2Afo), *Stephanodiscus medius* Håkansson (2Sme), rarely chrysophyte cysts (2CC), and *Cyclotella pseudostelligera* Hustedt (2Cps). These species are known to preferencially occur during the transition from spring circulation to summer stratification (Kling 1993; Ringelberg 1997; Interlandi et al. 1999; Raubitschek et al. 1999). *C. comensis* typically forms vernal blooms in clear, well-mixed, and oligotrophic lakes (Reynolds et al. 2002). *A. formosa* prefers enhanced concentrations of P, N and Si (Interlandi et al. 1999). The species is known to

tolerate light deficiency, but blooms terminate when the water column stratifies, already before decreasing Si concentration become limiting (Neale et al. 1991; Reynolds et al. 2002). Because *S. medius* is often mixed with *S. minutulus* (Krammer and Lange-Bertalot 1991a) it is difficult to classify. According to this authors, the species prefers eutrophic waters.

The long, fragile *Fragilaria tenera* (W. Smith) Lange-Bertalot (synonymous with *Synedra acus* Hustedt) (3Fte) occurs with massive bloom layers in the younger part of the sequence. This species is known to bloom with the onset of stratification of the water column in early summer (Interlandi et al. 1999; Rosén et al. 2000), where it withstands the grazing pressure of zooplankton because of its large size and needle-like shape (Sommer 1988). It is a good competitor for P and prefers enhanced N-concentrations under Si-saturated conditions (Interlandi et al. 1999). In rare years, we observed layers of *Synedra ulna* (Nitzsch) Ehrenberg (3Sul), *Fragilaria crotonensis* Kitton (3Fcr), or chrysophyte cysts (3CC).

In late-summer or early-fall, with increasing mixing depth, nutrients are recycled from the hypolimnion and favour a further bloom of diatoms (4FB) (Sommer et al. 1986). Small, fast growing centrics (*C. comensis* – 4Cco) are the first to respond to the re-availability of nutrients (Raubitschek et al. 1999). Also species present during spring circulation, such as *A. formosa* (4Afo) or *A. subarctica* (4Asu) can form a second bloom during the fall (Interlandi et al. 1999). In a number of years, they co-occur with the large centric *Punctinella radiosa* Grunow, Håkansson (4Pra), which can survive with reduced light levels (Sommer et al. 1986).

Mixed with the diatoms blooming at the onset of the fall circulation, or as a distinct sublamina in fall, are fine-silt-sized detritus (4F). Towards the termination of that layer, the percentage of organic and clastic detritus increases, forming a transition to the fall-circulation layer. An increased detritus grain size is then the characteristic of the fall circulation layer (5FC). In contrast to the spring circulation layer, the fraction of organic detritus is enhanced. The terminations for the varves are the winter deposits, consisting mainly of fine, dispersed, organic detritus in a clay matrix (6WCl).

Deviations from the above described varve microfacies may be either the lack of certain sublaminae or the occurrence of additional sublaminae. The latter are, for example, clayey layers rich in fine, dispersed organic particles. They may be related to blooms of algae, not forming preservable remains, that replaced diatoms in the plankton succession. A second, frequently observed type of additional sublaminae are layers rich in detritus, but with a smaller grain size than the circulation layers, and a low fraction of, mainly littoral, diatoms. They are assigned to external input events, possibly strong rain, in spring and summer (Sp1, 3Su). Six of the sublaminae types, described above (in seasonal succession: 1SC, 1Sp, 3Su, 4F, 5FC, and 6WCl) consist mainly of clastic and organic detritus and are of allochthonous origin. The remaining layers consist mainly of planktonic diatoms and are of biogenic, autochthonous origin.

The most conspicuous layers are turbidites, consisting almost exclusively of clastic detritus graded from fine sand at the base to clay at the top. These sediments originate from turbidity currents, caused by events in the lake catchment leading to down-slope movement of sediment. As Lake Holzmaar is only peripherally influenced by a brook (Sammetbach, see Figure 1), such events are probably heavy rain or snow melt that can trigger slope slides or enhance input from surface run-off, especially when vegetation is sparse or perturbed (e.g., Sletten et al. 2003). Because the turbidites do not belong to the annual course of sedimentation, they were excluded from the varves.

The quality of the varves is best characterized by the presence of distinct sublaminae types, classified seasonally and, according to the phase of the thermal regime (Figure 3), i.e. the circulation layers of spring and fall, the winter clay layer, and the bloom layers of spring, summer, and fall. The presence of at least two such layers provides sufficient indication for identifying them as one varve. This criterion is not fulfilled in 10 out of 336 cases, which suggests a possible error of 3%.

Chronology

The cores HZM 41A and HZM 42B were selected for the varve study of the uppermost part of the

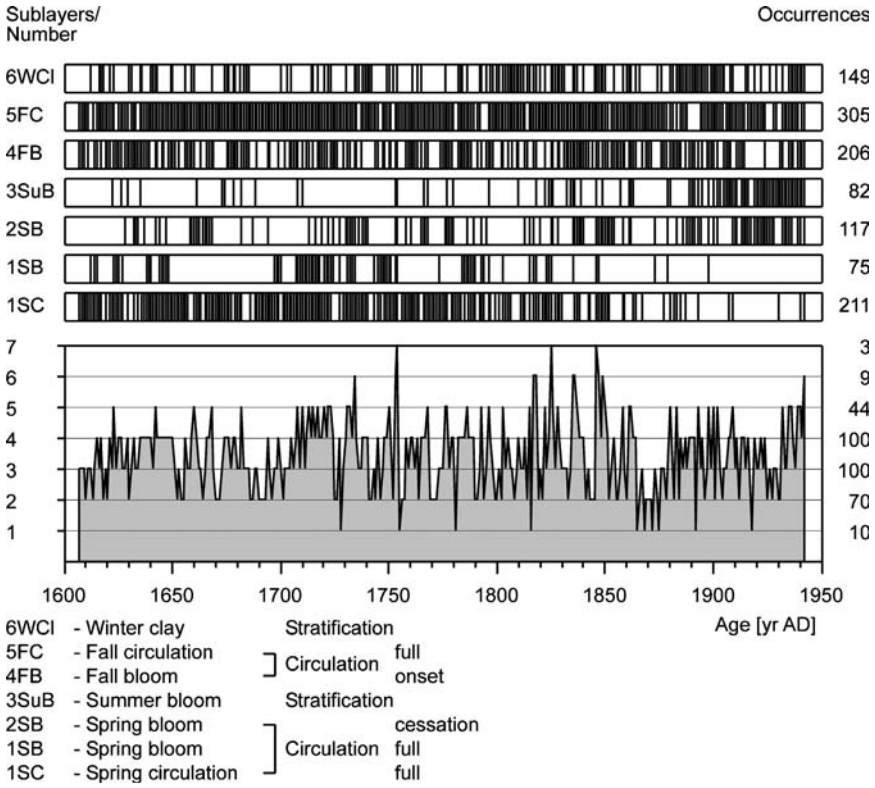

Figure 3. Presence, number and distribution of distinct sublaminae in the varves of Lake Holzmaar as a measure for their quality in relation to the reliability of the chronology (for sublaminae coding, see Table 4).

sequence, because of the preservation of varves and their high quality. For the chronology, they were visually correlated using a section of 30 years with 12 years below and 18 years above the turbidite marker layer M2 (in Figure 4a). The chronology for the sequence is floating because the uppermost 23 cm sediment do not show traceable varves. The varved sequence comprises 336 years. In order to fix the chronology, we applied linear regression using the depth of the base of each varve (Figure 4a). This is justified by the time series' overall linear behavior, which is substantiated by the high coefficient of determination in linear regression ($R^2 = 0.99$). For calculation purposes, the sediment surface was set to AD 2000 (coring date summer 1999). The best fit, i.e. when the calculated sediment depth at AD 2000 is zero, resulted when the studied sequence was fixed to the period AD 1607–1942. Then, the linear regression over the last seven varves (AD 1936–1942) results in a coefficient of determination equal to one and a sediment depth at AD 2000 equal to zero centimeters. The increase of thickness of this varves may reflect an influence of porosity on the varve thickness. According to the regression equation, the sedimentation rate is 4.05 mm yr^{-1}. Although the varves are disturbed in the top 23 cm of HZM 41, the sedimentation rate of 4.5 mm yr^{-1}, calculated from the ^{210}Pb-activity profile of unsupported ^{210}Pb according to Appleby (1993), supports our chronology (Figure 4b).

For three out of five samples dated by AMS ^{14}C-dating, the estimated ages are too young compared with the ages from the varve chronology (Figure 4, Table 3). These dates are difficult to interpret, as the presence of intact varves confirms that no physical contamination of the sediments by recent organic material occurred. A potential reason for these young ages is the absorption of modern CO_2 from the storage environment (water or remaining air in the bottle) by fungi or microorganisms, which may easily be incorporated into a sample during preparation and identification of the organic remains (Wohlfarth et al. 1998b). Consequently, a long storage time (> 6 months) is considered to result in radiocarbon ages that are

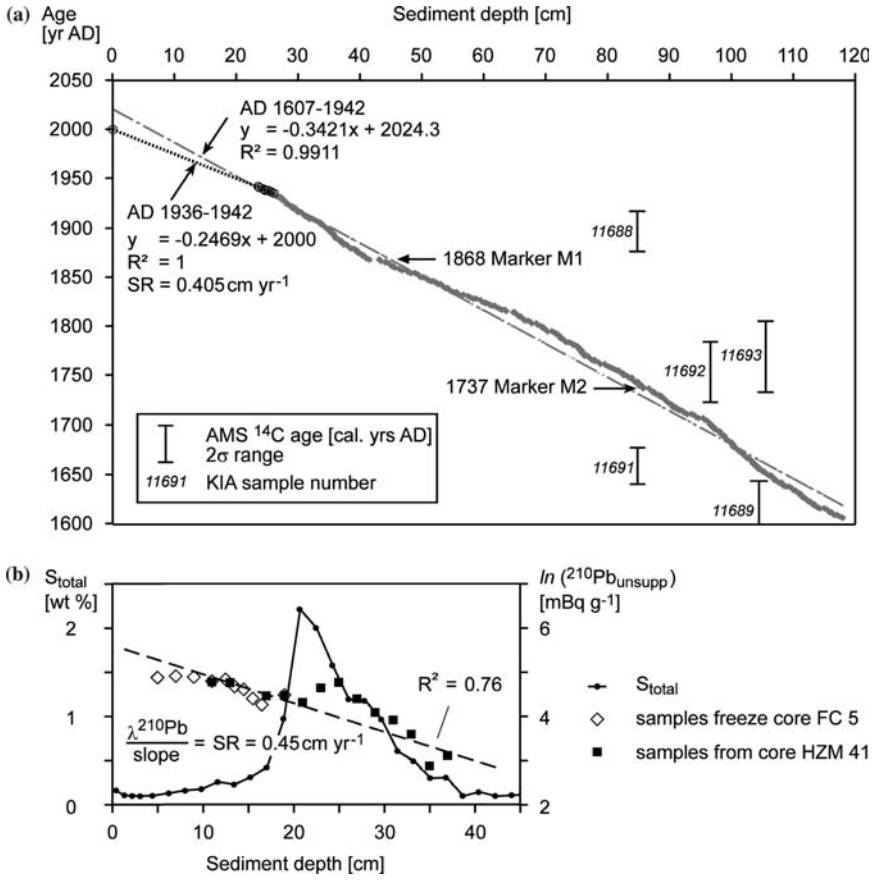

Figure 4. (a) Age-depth-relations for the sequence HZM 41/42 from Lake Holzmaar, estimated AMS ^{14}C-ages and linear regression: gray diamonds and gray dash-point line for the period AD 1607–1942; black circles and black dashed line for the period AD 1937–1942. (b) Semi-logarithmic plot of $^{210}Pb_{unsupp}$ versus depth. The profile of total sulfur documents the recent eutrophication of Lake Holzmaar. The $^{210}Pb_{unsupp}$-plateau around 20 cm depth probably reflects the bulk effect of temporarily enhanced mass accumulation and diffusive redistribution of ^{210}Pb (Schettler, unpublished data). The given ^{210}Pb activity values are related to September 21, 2000.

too young (Wohlfarth et al. 1998b). For the material at hand, the storage time of the core (at 4 °C) before sampling was 10 months. An additional 7 months (mainly at 4 °C in aqua dest.) passed before the samples were dated. The older ages of KIA11689 and KIA11691 may be related to reworking. For the latter sample this is highly probable as it was taken from a turbidite layer. In conclusion, the estimated ^{14}C-ages do not provide the basis for a consistent chronology for a floating varve series which is temporally precise in itself.

Varve variables

Varve thickness ranges between 0.4 mm and 7.1 mm with an average of 2.64 mm (Figure 5). The sequence contains seventeen turbidites ranging in thickness from 0.5 to 14.5 mm. The varve thickness record shows one distinct phase with below-average values from AD 1645–1705 and one distinct phase with above-average values from AD 1815–1870.

The thickness of all 13 sublaminae that pass the cut-off criterion of $N = 33$ (=10%) occurrences are shown in Figure 6. For those, standard deviations in the thickness range between 0.073 and 0.631 mm.

Statistical analyses

DCA of the sublaminae thickness data with detrending by segments results in a gradient length of 3.4 SD for the first DCA-axis. Because this gradient length indicates a unimodal response in the

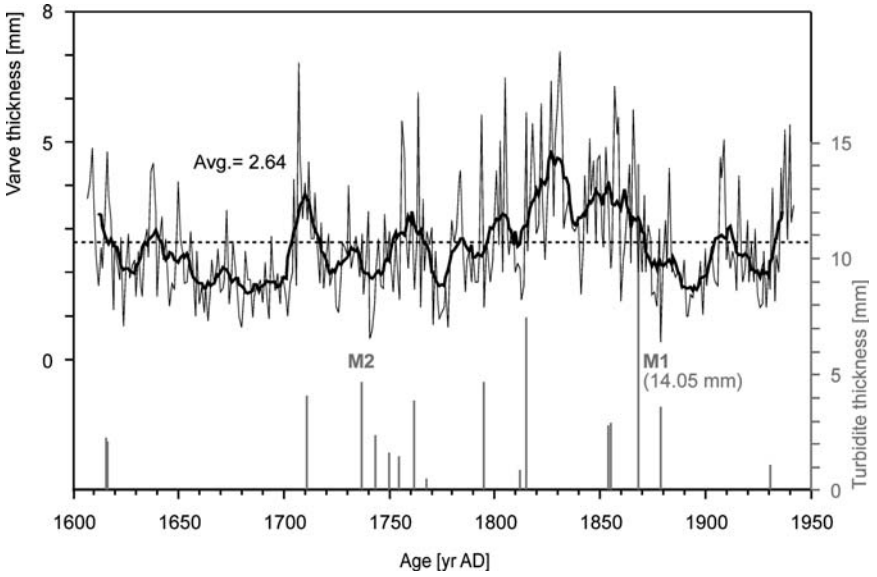

Figure 5. Varve thickness, sedimentation rate, turbidite and marker layers, respectively in the composite profile HZM 41/42 from Lake Holzmaar.

Holzmaar data, we applied indirect gradient analysis based on a unimodal response model, i.e. CA, for analysing the data structure (ter Braak and Prentice 1988). This was appropriate, as no arch effect was discernable in the CA sample scores.

The results of the CA are given in Table 5. In this study, the terminus 'species' of the ordination vocabulary refers to the respective varve sublamina, while 'sample' denotes the respective annual layer consisting of the thicknesses of all sublaminae. The first two CA-axes account for 29.6% of the total variation in the species and both explain an almost equal percentage of variance. Species scores away from the center of the biplot (Figure 7), (*2Sme, 3Fte*, 1Sp, 4F, and *1Asu*) do not in all cases depict low occurrence or small thickness of the sublamina, as indicated by the *N*-value (Table 4).

The 336 sample labels are omitted for clarity, but also because their arrangement does not appear to bear any temporal relation. In order to analyze the structure of the sample scores in relation to time, fuzzy c-means (FCM) cluster analysis was applied to the data set. As distance measure 'diagonal' was chosen, where the squared distance from a sample to the center of cluster is weighted by a matrix in diagonal norm (Bezdek et al. 1984). This results in the transformation of the sublaminae-thickness data into equal variance. Statistical models with the number of clusters from 2 to the maximum of 12 have been calculated. The number of valid clusters has been determined using the separation distance between the cluster (S_{dist}), the fuzziness performance index (*FPI*), and the modified partition entropy (*MPE*) (Figure 8a). The separation into 3 and 4 clusters with a fuzzy exponent ϕ of 1.2 leads to a drop in S_{dist} followed by an increase. While the values of *FPI* and *MPE* are still high for 3 clusters, they drop considerably for 4 clusters and again increase for 5 clusters in *FPI*. Minimum values of validation parameters are obtained for separation into 8 clusters. The overlap between the clusters has been estimated using the confusion index *CI* (Bezdek 1984). Thereby, a small *CI* indicates samples that are mainly members of one cluster (Figure 8b). Repetitions of the FCM clustering with the same parameters with random start showed the stability of the separation into 4 clusters. The separation into four clusters was additionally preferred because of the temporal coincidence of the stable phases of the

Table 5. Results of the CA with the eigenvalues ($\lambda_1,\ldots,_4$) of the first four ordination axes, the sum of all eigenvalues ($\sum \lambda_i$) and the cumulative percentage of explained variance (CVP).

	λ_1	λ_2	λ_3	λ_4	$\sum\lambda_i$
	0.32	0.31	0.24	0.22	2.15
CVP (%)	15.1	29.6	41	51.2	

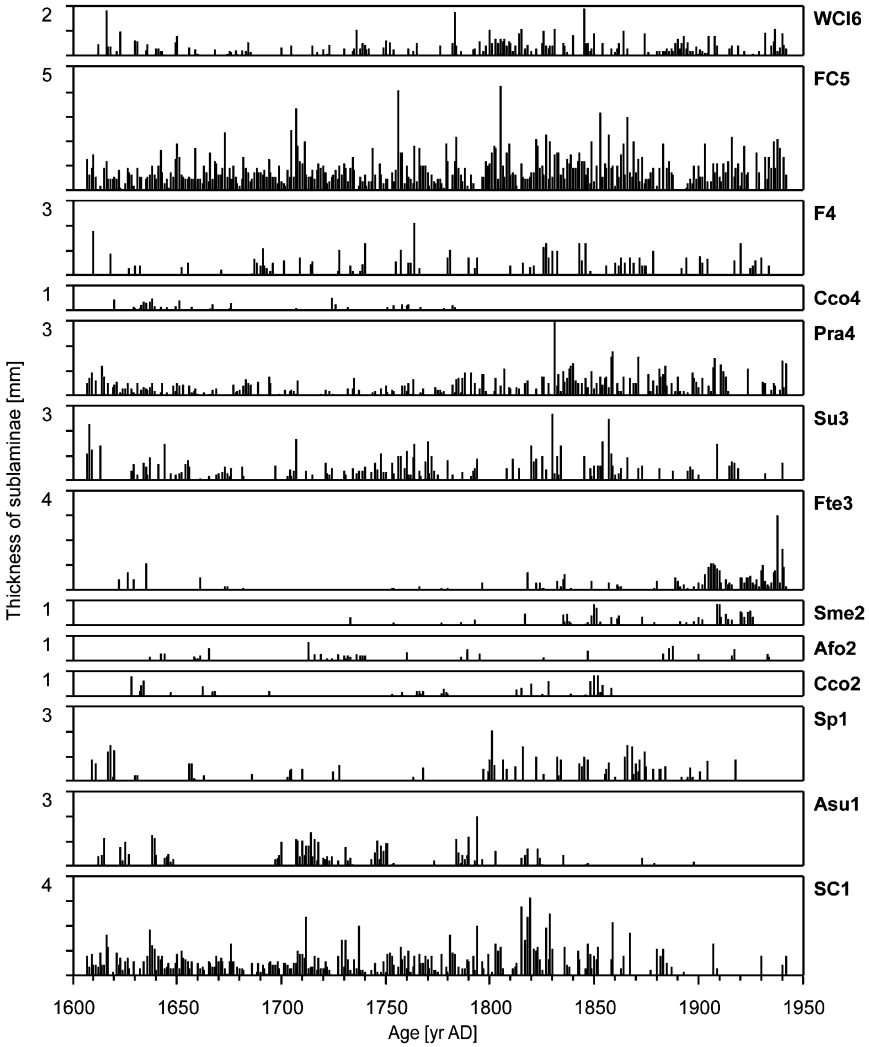

Figure 6. Thickness of sublaminae that passed the cut-off criterion of 10%-occurrence. For explanation of codes, see Table 4.

four clusters with periods in the regional historical development (see below) and because of the lack in stability in the 8 clusters.

The plot, showing the allocation of the annual layers to this 4 clusters along the time axis (Figure 9), indicates stable states, i.e. assignment of the samples to mainly one cluster, for the entire sequence. The symbols assigned to the samples of each cluster in this diagram, are also used in the CA biplot (Figure 7). These clusters are ordinated in the biplot according to the sample scores such that cluster 1 samples plot in the center, while those of the second, third and fourth clusters have scores mainly in the third, fourth, and first quadrants of the biplot, respectively.

Discussion

Patterns in the combined sublaminae thickness data

The inter-species distance plot of the first two CA-axes (Figure 7) shows an almost clear separation of diatom bloom layers and non-bloom layers along CA-axis 2, i.e. bloom layers (italics) have negative species scores and non-bloom layers (clastic or detritus layers) have positive scores on axis 2 with the exception of 1SC. The species score of 1SC close to those of *2Afo* and *2Cco* depicts the association of spring circulation sublaminae with spring diatom blooms related to a circulation regime. The similar score of the spring-blooming

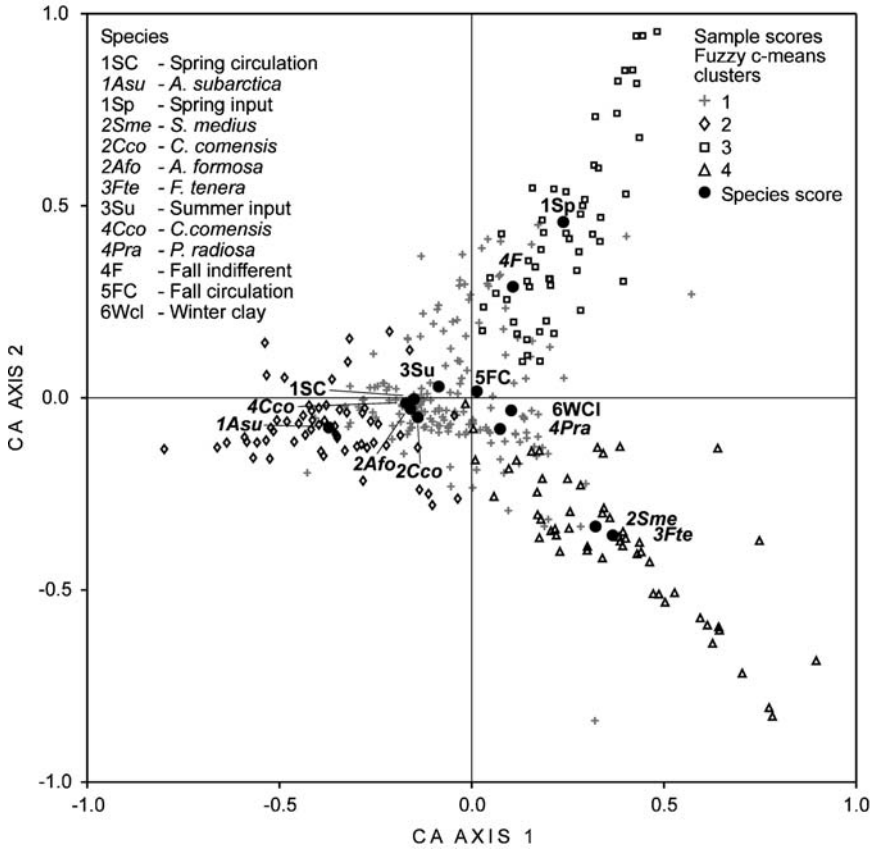

Figure 7. Correspondence analysis, inter-species distance plot. Symbols for samples refer to clusters derived from fuzzy c-means clustering.

2Cco and the fall-blooming *4Cco* may be because the species shows blooms both in spring and in fall (Raubitschek et al. 1999). The location of the species score of the spring-blooming *A. subarctica* (*1Asu*) away from the origin may result not only from the slightly lower *N*-value, but also from the distinctly different ecological preferences of the species, characterized as 'nordic-alpine' (Krammer and Lange-Bertalot 1991a). Autecological studies relate its occurrence to lower temperatures and ice cover, relatively low-light conditions (Gibson and Fitzsimons 1990; Siver and Kling 1997; Interlandi et al. 1999) and increased turbulence (Lund 1971). Periods of the species' occurrence can be thus characterized as cooler with prolonged spring circulation.

The sublaminae deposited under a weakly turbulent regime and those formed under a more turbulent regime are separated along CA-axis 1 with the former preserving positive CA1-scores and the latter receiving negative CA1-scores. Besides 1SC, *1Asu*, *2Afo, 2Cco*, and *4Cco*, 3Su belongs to the sublaminae formed under a more turbulent regime. Strong rain events typically occurring in the low-mountain-range region during summer may be responsible for the formation of the 3Su sublamina. The score of the fall-circulation lamina 5FC close to the center of the plot originates from the large *N*-value and from the ubiquity of the sublamina in the varves.

Clastic-organic sublaminae formed under a weakly turbulent or stagnant regime are 6WCl, 1Sp, 4F. In comparison to 6WCl, the winter clay that is likely to be deposited under the ice cover, 1Sp and 4F denote sediments of fine to middle silt grain size with mainly littoral diatoms (less than 25%). In a number of years, these layers substitute the bloom layers of the respective season. They may originate from the settling of fine particles under calm water conditions or represent redeposition. In the case of 4F, the depositional mechanism is likely to be settling after the break-down of

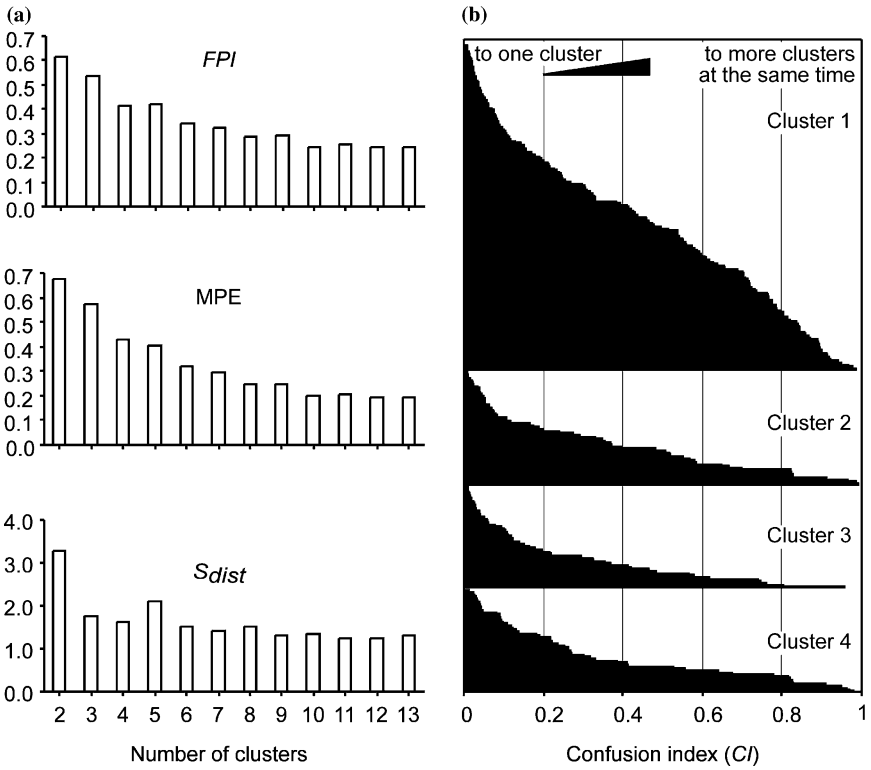

Figure 8. Summary data of the fuzzy c-means cluster analysis. (a) Separation distance between the cluster (S_{dist}), fuzziness performance index (*FPI*), and modified partition entropy (*MPE*), (b) Confusion index (*CI*) as measures for the validity of the number of clusters.

summer stratification. Diatom blooms classified as deposited under calm water conditions (*2Sme, 3Fte*, *4Pra*) occur at the onset, during or at the break-down of summer stratification. *S. medius* and *F. tenera* (synonymous with *Synedra acus* Hustedt), additionally have higher nutrient requirements (Krammer and Lange-Bertalot 1991a). Interlandi et al. (1999) found preferences of *Synedra* species to high N:P ratios. The occurrence of massive bloom layers of *S. medius* after AD 1830 and of *F. tenera* after AD 1880 may therefore be related also to enhanced concentrations of P and N.

Temporal structures and implications for climatic and anthropogenic influence

While CA ordinates the combination of the sublaminae thickness data in the respective varves (years), FCM clustering reveals the temporal distribution of the clusters of the combined sublaminae thickness data. By symbolizing the sample scores in the CA biplot (Figure 7) according to the FCM clusters in which they occur (Figure 9), the combination of the important sublaminae in a respective cluster is visualized (see legend for sample scores on Figure 9). Most years (170) belong to cluster 1 and show scores in the center of the CA biplot. These scores are associated with the sublaminae with the largest *N*-values (1SC, 3Su, *4Pra*, 5FC, 6WCl) that are mainly of clastic origin. Cluster 2 combines essentially the years with spring-bloom layers of *A. subarctica* (*1Asu*) associated with strong turbulence, low-light, and lowered temperatures. Cluster 3 incorporates the diatom-bloom sublaminae related to summer stratification with preference for higher nutrient concentrations (*2Sme, 3Fte*). The sublaminae 1Sp and 4F that originate from external input or redeposition, related to rain or water agitation, aggregate in cluster 4. Using the information from the sublaminae combinations on thermal and hygric conditions, nutrient concentration, and strength of external input, the years assigned to a respective cluster can be characterized in that

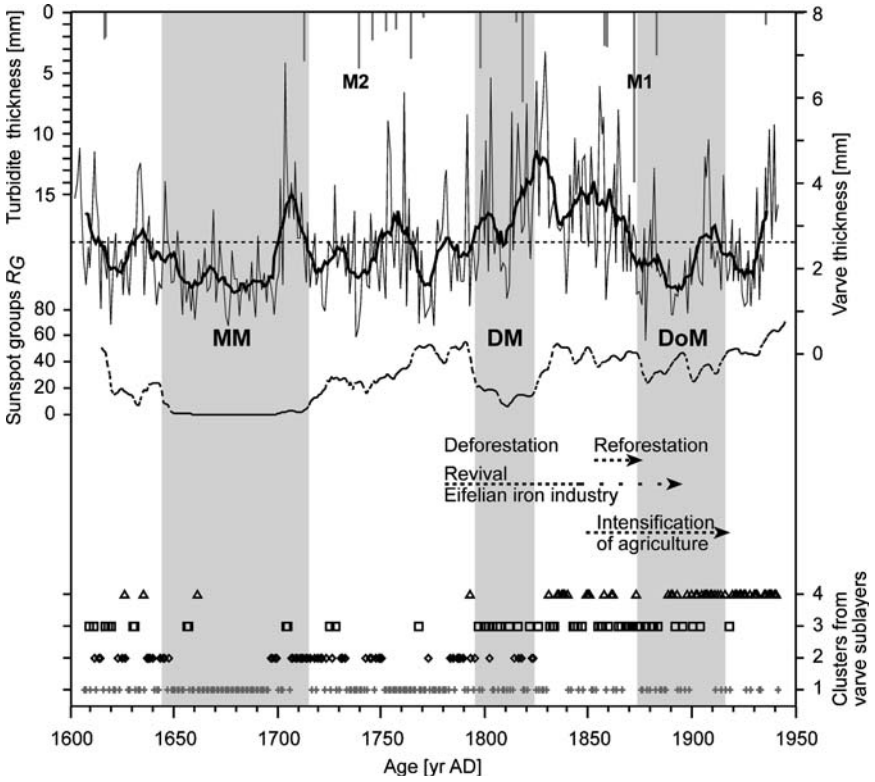

Figure 9. Clusters resulting from the fuzzy c-means clustering plotted along the time axis compiled with turbidite thickness and varve thickness (11-point running mean), the 11-point running mean of the sunspot group number (Hoyt and Schatten 1998) and implications for climatic and anthropogenic influences.

terms. This characterization of the clusters with respect to limnic processes, diatom patterns, varve thickness, external input and their relation to anthropogenic and climatic influences in the given temporal frame (AD 1607–1942) is summarized in Table 6.

Cluster 1-samples have a strong external input component with increased grain size of the clastic component mainly in 1SC sublaminae. This may be related to snow-melt induced strong and long-lasting spring circulation, which leads to late and weak or even absent summer stratification. Diatom blooms are almost exclusively blooms of *Punctinella radiosa*, with enhanced Si-demand (Interlandi et al. 1999), in fall. Stable cluster 1-phases occur from AD 1650–1700 and from AD 1750–1785. The first phase coincides with below-average thicknesses of the varves and, in time, with the Maunder Minimum in sunspots (MM) (Eddy 1976; Hoyt and Schatten 1998). Such proxy data evidence is the expression of cold air in winter, cold springs with southward shift of the mid-latitude storm tracks, and cooler and wetter summers, which are recorded and reconstructed especially for the Late MM (e.g., Manley 1974; Briffa et al. 1998; Fischer et al. 1998; Pfister 1999; Luterbacher et al. 2001; Zorita et al. 2004). Low production of exclusively fall-blooming diatoms, with an absence of spring blooms in the Holzmaar sequence, either indicates a shift of diatom production to fall, or the 'earlier' occurrence of fall conditions. The latter is a direct consequence of wetter and slightly cooler summers and autumns exhibiting advanced changes from summer to winter circulation during the Late MM (Luterbacher et al. 2001).

The association of **cluster 2**-samples is characterized by varves with a low detritus content and around-average thickness, which is dominated by thick spring layers. These include massive blooms of the nordic-alpine *A. subarctica*, a species with a preference for turbulent regimes and tolerance to low light conditions (e.g., Lund 1971; Interlandi et al. 1999). *A. subarctica* dominates the diatom production that is shifted to the period of a

Table 6. Characteristics of the clusters from the combination of the sublaminae thickness data in the varves of the Holzmaar sequence and implications concerning anthropogenic influences and climate linkages. (the dates are given in year AD)

Cluster	Diatom patterns	Varve thickness	External input	Stable phases	Limnic processes	Anthropogenic influences	Climatic linkages
1	Diatom blooms almost exclusively in fall (*Punctinella radiosa*)	Below average	Strong input of clastic and organic detritus in circulation layers in spring and fall	1650–1700	Strongly turbulent regime	Not evident	Maunder Minimum (1645–1715)
				1750–1785	Weak summer stratification		
2	Massive blooms of *Aulacoseira subarctica* in spring	Around average, determined by thickness of spring bloom layer	Decreased	(1610–1650)	Prolonged, strong spring circulation	Not evident	Onsets + Terminations of Maunder and Dalton Minima
				1700–1750	Weak summer stratification		
				1785–1795 1815–1825			
3	Diatom blooms mainly in fall (*Punctinella radiosa*)	Above average	Input throughout the year	1795–1815	Weak spring circulation	Deforestation	Dalton Minimum (1795–1825)damped by erosion
		Decrease centered around AD 1810	Dominance of small-grain-sized spring (1Sp) and fall (4F) layers	1825–1885	Weak summer stratification with rapid break down Strong fall circulation		
4	Massive blooms of *Stephanodiscus medius* and *Fragilaria tenera* with enhanced nutrient demand and high temperature optimum (*F. tenera*)	Below average, lowest around AD 1895	Lowest	1885–1942	Circulation mainly in fall	(Natural reforestation of the catchment)	Damon Minimum (centered at about 1900)
			Rare spring circulation layers		Stable and longer summer stratification periods	Nutrient input from artificial fertilizers	Onset of modern warming

prolonged spring circulation followed by short summers. These conditions determined the varve structure during four periods: from AD 1610–1650, AD 1700–1750, AD 1785–1795, and AD 1815–1825 framing the colder stable cluster 1-phases as transition periods.

In contrast to the MM with below-average VT, VT during the Dalton Minimum (DM) increases, interrupted only by a short drop centered around AD 1810. The respective sublaminae composition is summarized in **cluster 3** with stable phases between AD 1795–1815 and AD 1825–1885. Cluster 3-samples preserve a high external input throughout the year, which is attributable to a less energetic regime than that for clusters 1 and 2. The indication for this is the dominance of the lower grain-sized sublaminae in spring and fall (1Sp and 4F). Diatom blooms are, as in cluster 1, shifted to fall. Taken together this could be the result of increased soil erosion, which in turn may be due to disturbances of the vegetation cover following climate deterioration or human activities. Cold summers in the year after the Tambora eruption (AD 1816) (reported e.g., through low tree-ring density; Briffa et al. 1998; Crowley 2000), affected the Eifel region through crop failure in AD 1816 and 1817 (Blum 1925). The lower temperature decrease during the DM, compared to that during the MM (Jones 1988; Pfister 1999; Glaser 2001) however, makes a climatic origin for a disturbance of the vegetation unlikely. The probable reason for the enhanced external input is, as documented in several almanacs from the district of Daun, a reckless deforestation of the region that led to wasteland formation by the end of the 18th century (Blum 1925; Wenzel 1962; Schwind 1983). The iron industry, that had a sharp production increase in the 18th century, had to be provided with charcoal (Blum 1925; Wenzel 1962). In 1794, the climax was reached with the French occupation, which opened a considerable market for armaments. This massive human interference dampens the climate signal from the DM in the varves, which should be, similar to the MM, i.e. a below average VT.

Cluster 4-varves occur frequently after 1830 and in a stable manner after AD 1885 until the end of the record at AD 1942. They are characterized by below-average VT, the lowest external input in the sequence, and massive blooms of *Stephanodiscus medius* and *Fragilaria tenera*. The differences between the previous clusters and the cluster 4 are that the varves in the latter are dominated by sublaminae formed in a less energetic environment with enhanced nutrient concentrations. Possible reasons for this changed conditions are documented in historical records.

With the onset of the Prussian Era (after 1815), re-forestation of the region with primarily *Picea* was funded by the Prussian Eifel Cultural Fund from 1854–1871 (Wenzel 1962; Schwind 1983). For the Holzmaar catchment, however, natural reforestation of *Fagus*, as indicated by the modern stands of 144–172 years old *Fagus* and only solitary *Picea* trees, lead to the decrease in soil erosion (internal documents from the forestry office in Gillenfeld, and Breitenbach, personal communication).

Both blooming diatom species, *S. medius* and *F. tenera*, prefer enhanced nutrient concentrations. *Fragilaria tenera* is ranked at the upper end of the N gradient (Interlandi et al. 1999). The massive blooms of *F. tenera* beginning at the end of the 19th century may be related to the intensification of the outdated agriculture and the utilization of artificial fertilizers under the Prussian regime after 1850 (Blum 1925). This is the point at which cluster 4-samples appear increasingly in the sequence. Additionally, *Fragilaria tenera* has a high temperature optimum (Rosén et al. 2000) and the massive blooms suggest stable and longer summer stratification periods of the water column. This may be a first indication of the modern warming trend in Lake Holzmaar as inferred by e.g., Jones et al. (1998) and Mann et al. (1999). At the onset of this trend, a drop in VT centered around AD 1890 and recurring cluster 1-conditions may indicate the Damon Minimum (Jones 1988; Hoyt and Schatten 1998).

Conclusions

Varve microfacies analyses revealed 21 different varve sublaminae in the sediment sequence from Lake Holzmaar (Eifel, W-Germany). Using linear regression, the varved sequence, that terminates at 23 cm sediment depth below the core top, is dated to the period AD 1607–1942. The sedimentation rate for the non-varved top layer, derived from the regression equation, is corroborated by that calculated from ^{210}Pb activities.

Correspondence analysis and fuzzy c-means clustering were used to extract patterns in the annually combined sublaminae data, including thickness, lithology, fabric, and microfossil content. The partitioning of the samples (years) into four clusters, each related to thermal and hygric conditions and/or human activities, tracks the development of Lake Holzmaar and its catchment from AD 1607–1942, which is in temporal agreement with historical and instrumental records. Samples in clusters 1 and 2 clearly show the influence of colder climatic conditions. Cluster 1-samples indicate colder and wetter conditions, especially during a stable phase from AD 1650–1700, coinciding with the Maunder Minimum (MM). Cluster 2-conditions (vigorous and prolonged spring turnover with massive blooms of the nordic-alpine *A. subarctica*) represent the climatic transition to those of cluster 1.

The samples assigned to clusters 3 and 4 reflect anthropogenic influences. Cluster 3 (AD 1795–1815 and AD 1825–1885) combines above-average VT and high, but less energetic, external inputs throughout the year. The climatic signal of a colder Dalton Minimum (short drop in VT centered around AD 1810) is superimposed by increased input from soil erosion. The latter is related to widespread deforestation of the region originating from the demand for charcoal by the Eifelian iron industry, which experienced a sharp increase in production at the end of the 18th century. At AD 1885, cluster 3-conditions become the stable state in Lake Holzmaar. This is a less energetic environment with enhanced nutrient concentration, resulting form the lake's response to natural reforestation of the *Fagus* stands in the catchment and the use of artificial fertilizers, both starting in the 1850s in the Eifel. The longer thermal stratification periods suggested by summer blooms of diatoms may indicate the onset of the modern warming trend. At the beginning of the cluster 4-period, a drop in VT centered around AD 1890 and recurring cluster 1-conditions may be related to the Damon Minimum.

Acknowledgments

Financial support for this study was provided through the DFG project Ki 612/6. We would like to thank the co-workers of the section 'Climate dynamics and Sediments' at the GeoForschungs-Zentrum Potsdam who carried out the coring and sample preparation. The drilling was a contribution to the project KIHZ (Natürliche Klimavariationen in historischen Zeiten), funded by the 'Helmholtz-Gemeinschaft'. S. Prasad, G. Yanchva, A. Brauer and T. Kumke and two anonymous reviewers are acknowledged for their helpful comments on the manuscript. Valuable personal communications came from A. Lücke and R. Breitenbach. We thank J.F.W. Negendank who encouraged this study and initiated the study of the German maar lakes.

References

Alefs J. and Müller J. 1999. Differences in the eutrophication dynamics of Ammersee and Starnberger See (Southern Germany), reflected by the diatom succession in varve-dated sediments. J. Paleolimnol. 21: 395–407.

Anderson R.Y. and Dean W.E. 1988. Lacustrine varve formation through time. Palaeogeogr. Palaeocl. 62: 215–235.

Appleby P.G. 1993. Forward to the lead-210 dating anniversary series. J. Paleolimnol. 9: 155–160.

Baier J., Negendank J.F.W. and Zolitschka B. 2004. Mid- to Late Holocene lake ecosystem response to catchment and climatic changes - a detailed varve analysis of Lake Holzmaar (Germany). In: Miller H., Negendank J.F.W., Flöser G., von Storch H., Fischer H., Lohmann G. and Kumke T. (eds), The Climate in Historical Times – Towards a Synthesis of Holocene Proxy Data and Climate Models. Springer-Verlag, Berlin, pp. 195–208.

Bard E., Raisbeck G., Yiou F. and Jouzel J. 2000. Solar irradiance during the last 1200 years based on cosmogenic nuclides. Tellus 52B: 985–992.

Battarbee R.W. 2000. Palaeolimnological approaches to climate change, with special regard to the biological record. Quatern. Sci. Rev. 19: 107–124.

Bezdek J.C., Ehrlich R. and Full W. 1984. FCM: the fuzzy c-means clustering algorithm. Comp. Geosci. 10: 191–203.

Blum P. 1925. Entwicklung des Kreises Daun. Verlag des Kreisausschusses, A. Schneider, Daun. 324 pp.

Bradbury J.P. 1988. A climatic-limnologic model of diatom succession for paleolimnological interpretation of varved sediments at Elk Lake, Minnesota. J. Paleolimnol. 1: 115–131.

Bradbury J.P., Colman S.M. and Reynolds R.L. 2004. The history of recent limnological changes and human impact on Upper Klamath Lake, Oregon. J. Paleolimnol. 31: 151–165.

Brauer A., Litt T., Negendank J.F.W. and Zolitschka B. 2001. Lateglacial varve chronology and biostratigraphy of lakes Holzmaar and Meerfelder Maar, Germany. Boreas 30: 83–88.

Brauer A. 2004. Annually laminated lake sediments and their palaeoclimatic relevance. In: Miller H., Negendank J.F.W., Flöser G., von Storch H., Fischer H., Lohmann G. and Kumke T. (eds), The Climate in Historical Times – Towards

a Synthesis of Holocene Proxy Data and Climate Models. Springer-Verlag, Berlin, pp. 109–128.
Briffa K.R., Jones P.D., Schweingruber F.H. and Osborn T.J. 1998. Influence of volcanic eruptions on Northern Hemisphere summer temperature over the past 600 years. Nature 393: 450–455.
Büchel G. 1993. Maars of the Westeifel. In: Negendank J.F.W. and Zolitschka B. (eds), Paleolimnology of Eifel Maar Lakes. Springer, Berlin, Heidelberg, pp. 1–13.
Crowley T.J. 2000. Causes of climate change over the past 1000 years. Science 289: 270–277.
Dekkers M.J., Langereis C.G., Vriend S.P., van Santvoort P.J.M. and de Lange G.J. 1994. Fuzzy *c*-means cluster analysis of early diagenetic effects on natural remanent magnetisation acquisition in a 1.1 Myr piston core from the Central Mediterranean. Phys. Earth planet. In. 85: 155–171.
Eddy J.A. 1976. The Maunder Minimum. Science 192: 1189–1202.
Fischer H., Werner M., Wagenbach D., Schwager M., Thorsteinnson T., Wilhelms F., Kipfstuhl J. and Sommer S. 1998. Little ice age clearly recorded in northern Greenland ice cores. Geophys. Res. Lett. 25: 1749–1752.
Flynn W.W. 1968. The determination of low levels of polonium-210 in environmental materials. Anal. Chim. Acta 43: 221–227.
Gibson C.E. and Fitzsimons A.G. 1990. Induction of the resting phase in the planktonic diatom *Aulacoseira subarctica* in very low light. Br. phycol. J. 25: 329–334.
Glaser R. 2001. Klimageschichte Mitteleuropas. 1000 Jahre Wetter, Klima, Katastrophen. Wiss. Buchgesellschaft, Darmstadt, 227 pp.
Glenn C.R. and Kelts K. 1991. Sedimentary rhythms in lake deposits. In: Einsele G., Ricken W. and Seilacher A. (eds), Cycles and Events in Stratigraphy. Springer, Berlin, Heidelberg, pp. 188–221.
Hanesch M., Scholger R. and Dekkers M.J. 2001. The application of fuzzy *c*-means cluster analysis and non-linear mapping to a soil data set for the detection of polluted sites. Phys. Chem. Earth (A) 26: 885–891.
Hausmann S., Lotter A.F., van Leeuven F.N., Ohlendorf C., Lemcke G., Grönlund E. and Sturm M. 2002. Interactions of climate and land use documented in the varved sediments of seebergsee in the Swiss Alps. Holocene 12: 279–289.
Hill M.O. and Gauch H.G. 1980. Detrended correspondence analysis, an improved ordination technique. Vegetatio 42: 47–58.
Hoyt D.V. and Schatten K.H. 1998. Group sunspot numbers: a new solar activity reconstruction. Sol. Phys. 179: 189–219.
Interlandi S.J. and Kilham S.S. 1999. Responses of phytoplankton to varied resource availability in large lakes of the Greater Yellowstone Ecosystem. Limnol. Oceanogr. 44: 668–682.
Itkonen A. and Salonen V.-P. 1994. The response of sedimentation in three varved lacustrine sequences to air temperature, precipitation and human impact. J. Paleolimnol. 11: 323–332.
Jones P.D. 1988. Hemispheric surface air temperature variations: recent trends and an update to 1987. J. Climate 1: 654–660.
Jones P.D., Briffa K.R., Barnett T.P. and Tett S.F.B. 1998. High-resolution paleoclimatic records for the last millennium: interpretation, integration and comparison with general circulation model control-run temperatures. Holocene 8: 455–471.
Kelts K., Briegel U., Ghilardi K. and Hsü K. 1986. The limnogeology-ETH coring system. Schweiz. Z. Hydrol. 48: 104–115.
Kling H.J. 1993. *Asterionella formosa* RALFS: the process of rapid size reduction and its possible ecocogical significance. Diatom Res. 8: 475–479.
Krammer K. and Lange-Bertalot H. 1986. Bacillariophyceae (Naviculaceae). In: Ettl H., Gerloff J., Heynig H. and Mollenhauer D. (eds), Süßwasserflora von Mitteleuropa (1 (4)). Fischer, Stuttgart, 876 pp .
Krammer K. and Lange-Bertalot H. 1988. Bacillariophyceae (Bacillariaceae, Epithemiaceae, Surirellaceae). In: Ettl H., Gerloff J., Heynig H. and Mollenhauer D. (eds), Süßwasserflora von Mitteleuropa (2 (4)). Fischer, Stuttgart, 596 pp .
Krammer K. and Lange-Bertalot H. 1991a. Bacillariophyceae (Centrales, Fragilariaceae, Eunotiaceae). In: Ettl H., Gerloff J., Heynig H. and Mollenhauer D. (eds), Süßwasserflora von Mitteleuropa (3 (4)). Fischer, Stuttgart, 576 pp .
Krammer K. and Lange-Bertalot H. 1991b. (Bacillariophyceae Achnanthaceae, critical remarks to *Navicula*). In: Ettl H., Gerloff J., Heynig H. and Mollenhauer D. (eds), Süßwasserflora von Mitteleuropa (4 (4)). Fischer, Stuttgart, 437 pp .
Kumke T., Hense A., Schölzel C., Andreev A.A., Brüchmann C., Gebhardt C., Helle G., Kienel U., Kühl N., Neumann F. and Schleser G. 2004. Transfer functions for paleoclimate reconstructions – applications. In: Fischer H., Kumke T., Lohmann G., Flöser G., Miller H., von Storch H. and Negendank J.F.W. (eds), The Climate in Historical Times – Towards a Synthesis of Holocene Proxy Data and Climate Models. Springer-Verlag, Berlin, pp. 245–262.
Lean J. and Rind D. 1999. Evaluating sun-climate relationships since the Little Ice Age. J. Atmos. Sol.-Terr. Phy. 61: 25–36.
Legendre P. and Legendre L. 1998. Numerical Ecology. Elsevier, Amsterdam, 853 pp.
Lotter A.F. 1989. Evidence of annual layering in Holocene sediments of Soppensee, Switzerland. Aquat. Sci. 51: 19–30.
Lotter A.F. 1998. The recent eutrophication of Baldeggersee (Switzerland) as assessed by fossil diatom assemblages. Holocene 8: 395–405.
Lotter A.F. and Birks H.J.B. 1997. The separation of the influence of nutrients and climate on the varve time-series of Baldeggersee, Switzerland. Aquat. Sci. 59: 362–375.
Lotter A.F., Sturm M., Teranes J.L. and Wehrli B. 1997. Varve formation since 1885 and high-resolution varve analyses in hypertrophic Beldeggersee (Switzerland). Aquat. Sci. 59: 304–325.
Lücke A., Schleser G.H., Zolitschka B. and Negendank J.F.W. 2003. A lateglacial and Holocene organic carbon isotope record of lacustrine paleoproductivity and climatic change derived from varved lake sediment of Lake Holzmaar, Germany. Quatern. Sci. Rev. 22: 569–580.
Lund J.W.G. 1971. An artificial alteration of the seasonal cycle of *Melosira italica* subsp. *subarctica* in an English lake. J. Ecol. 59: 521–533.
Luterbacher J., Rickli R., Xoplaki E., Tinguely C., Beck C., Pfister C. and Wanner H. 2001. The Late Maunder Minimum (1675–1715) – A key period for studying decadal scale climatic change in Europe. Climatic Change 49: 441–462.
Manley G. 1974. Central England temperatures: monthly means 1659 to 1973. Q. J. Roy. Meteor. Soc. 100: 389–405.

Mann M.E., Bradley R.S. and Hughes M.K. 1999. Northern hemisphere temperatures during the past millennium: inferences, uncertainties, and limitations. Geophys. Res. Lett. 26: 759–762.

Merkt J. and Müller H. 1999. Varve chronology and palynology of the Lateglacial in Northwest Germany from lacustrine sediments of Hämelsee in Lower Saxony - a widespread isochronous late Quaternary tephra layer in central and northern Europe. Quatern. Int. 61: 41–59.

Neale P.J., Talling J.F., Heaney S.I., Reynolds C.S. and Lund J.W.G. 1991. Long-time series from the English Lake District: irradiance-dependent phytoplankton dynamics during the spring maximum. Limnol. Oceanogr. 36: 751–760.

Ohlendorf C., Niessen F. and Weissert H. 1997. Glacial varve thickness and 127 years of intstrumental climate data – a comparison. Climatic Change 36: 391–411.

Pfister C. 1999. Wetternachhersage. 500 Jahre Klimavariationen und Naturkatastrophen 1796–1995. Paul Haupt Verlag, Bern, Stuttgart Wien, 304 pp.

Ramstack J.M., Fritz S.C., Engstrom D.R. and Heiskary S.A. 2003. The application of a diatom-based transfer function to evaluate regional water-quality trends in Minnesota since 1970. J. Paleolimnol. 29: 79–94.

Raubitschek S., Lücke A. and Schleser G.H. 1999. Sedimentation patterns of diatoms in Lake Holzmaar, Germany - (on the transfer of climate signals to biogenic silica oxygen isotope proxies). J. Paleolimnol. 21: 437–448.

Renberg I. 1990. A procedure for preparing large sets of diatom slides from sediment cores. J. Paleolimnol. 4: 87–90.

Reynolds C.S., Huszar V., Kruk C., Naselli-Flores L. and Melo S. 2002. Towards a functional classification of the freshwater phytoplankton. J. Plankton Res. 24: 417–428.

Ringelberg J. 1997. Two examples of the interplay between field observations and laboratory experiments from 35 years of research with planktonic organisms. Aquat. Ecol. 31: 9–17.

Rosén P., Hall R.I., Korsman T. and Renberg I. 2000. Diatom transfer-functions for quantifying past air temperature, pH and total organic carbon concentration from lakes in northern Sweden. J. Paleolimnol. 24: 109–123.

Scharf B.W. and Menn U. 1992. Hydrology and morphometry. In: Scharf B.W. and Björk S. (eds), Limnology of Eifel maar lakes Ach. Hydrobiol. 38, pp. 43–62.

Scharf B.W. and Oehms M. 1992. Physical and chemical characteristics. In: Scharf B.W. and Björk S. (eds), Limnology of Eifel maar lakes, Ach. Hydrobiol. 38, pp. 63–83.

Schnurrenberger D., Russell J. and Kelts K. 2003. Classification of lacustrine sediments based on sedimentary components. J. Paleolimnol. 29: 141–154.

Schwind W. 1983. Der Wald der Vulkaneifel in Geschichte und Gegenwart. PhD thesis, Universität Göttingen, Forstwissenschaftlicher Fachbereich, 458 pp.

Shvetsov M.S. 1954. Concerning some additional aids in studying sedimentary formations. Bull. Moscow Soc. Nat. (Byull. Mosc. Obsshch. Isp. Prirody) 29: 61–66 (in Russian).

Siver P.A. and Kling H. 1997. Morphological observations of *Aulacoseira* using scanning electron microscopy. Can. J. Bot. 75: 1807–1835.

Siver P.A., Richard R., Richard G. and Giblin A.E. 2003. Estimating historical in-lake alkalinity generation from sulfate reduction and its relationship to lake chemistry as inferred from algal microfossils. J. Paleolimnol. 29: 179–197.

Sletten K., Blikra L.H., Ballantyne C.K., Nesje A. and Dahl S.O. 2003. Holocene debris flows recognized in a lacustrine sedimentary succession: sedimentology, chronostratigraphy and cause of triggering. Holocene 13: 907–920.

Smith S.V., Bradley R.S. and Abbott M.B. 2004. A 300 year record of environmental change from Lake Tuborg, Ellesmere Island, Nunavut, Canada. J. Paleolimnol. 32: 137–148.

Sommer U. 1988. Phytoplankton succession in microcosm experiments under simultaneous grazing pressure and resource limitation. Limnol. Oceanogr. 35: 1037–1054.

Sommer U., Gliwicz Z.M., Lampert W. and Duncan A. 1986. The PEG-model of seasonal succession of planktonic events in fresh waters. Arch. Hydrobiol. 106: 433–471.

Stoermer E.F. and Smol J.P. 1999. The Diatoms: Applications for the Environmental and Earth Sciences. Cambridge University Press, Cambridge, 469 pp.

Stuiver M. and Braziunas T.F. 1993. Sun, ocean, climate and atmosphere $^{14}CO_2$: an evaluation of causal and spectral relationships. Holocene 3: 289–305.

Stuiver M. and Polach H.A. 1977. Discussion: reporting of 14C data. Radiocarbon 19: 355–363.

Stuiver M., Reimer P.J., Bard E., Beck J.W., Burr G.S., Hughen K.A., Kromer B., McCormac F.G., v.d. Plicht J. and Spurk M. 1998. INTCAL98 radiocarbon age calibration 24,000–0 cal BP. Radiocarbon 40: 1041–1083.

Ter Braak C.J.F. 1994. Canonical community ordination. Part I: Basic theory and linear methods. Ecoscience 1: 127–140.

Ter Braak C.J.F. and Prentice I.C. 1988. A theory of gradient analysis. Adv. Ecol. Res. 18: 271–317.

Ter Braak C.J.F. and Smilauer P. 2002. CANOCO Reference Manual and User's Guide to Canoco for Windows: Software for Canonical Community Ordination (version 4.5). Microcomputer Power, Ithaca, NY, USA, 499 pp.

Terry R.D. and Chilingar G.V. 1955. Summary of "Concerning some additional aids in studying sedimentary formations." M.S. Shvetsov. J. Sediment. Petrol. 25: 229–234.

Tinner W., Lotter A.F., Ammann B., Conedera M., Hubschmid P., van Leeuwen J.F.N. and Wehrli M. 2003. Climatic change and contemporaneous land-use phases north and south of the Alps 2300 BC to 800 AD. Quatern. Sci. Rev. 22: 1447–1460.

Thienemann A. 1915. Physikalische und chemische Untersuchungen in den Maaren der Eifel. Verh. Naturhis. Ver. preuss. Rheinl. Westf. 71: 273–398.

Vriend S.P., van Gaans P.F.M., Middelburg J. and de Nus A. 1988. The application of fuzzy *c*-means cluster analysis and non-linear mapping to geochemical datasets: examples from Portugal. Appl. Geochem. 3: 213–224.

Wenzel I. 1962. Ödlandentstehung und Wiederaufforstung in der Zentraleifel. Arbeiten zur Rheinischen Landeskunde 18: 119.

Wohlfarth B., Holmquist B., Cato I. and Linderson H. 1998a. The climatic significance of clastic varves in the Ångermanälven Estuary, northern Sweden, AD 1860 to 1950. Holocene 5: 521–534.

Wohlfarth B., Skog G., Possnert G. and Holmquist B. 1998b. Pitfalls in the AMS radiocarbon-dating of terrestrial macrofossils. J. Quatern. Sci. 13: 137–145.

Zolitschka B. 1998. A 14,000 year sediment yield record from western Germany based on annually laminated lake sediments. Geomorphology 22: 1–17.

Zolitschka B., Brauer A., Negendank J.F.W., Stockhausen H. and Lang A. 2000. Annually dated Weichselian continental

paleoclimate record from the Eifel, Germany. Geology 28: 783–786.

Zolitschka B. and Negendank J.F.W. 1998. A high resolution record of Holocene palaeohydrological changes from Lake Holzmaar, Germany. In: Harrison S.P., Frenzel B., Huckriede U. and Weib M.M. (eds), Palaeohydrology as Reflected in Lake-level Changes as Climatic Evidence for Holocene Times. Fischer, Stuttgart, pp. 37–52.

Zorita E., von Storch H., Gonzalez-Rouco J.F., Cubasch U., Luterbacher J., Legutke S., Fischer-Bruns I. and Schlese U. 2004. Simulation of the climate of the last five centuries. Meteorol. Z. http://w3g.gkss.de/G/Mitarbeiter/storch/pdf/gkss_2003_12.pdf.